# Supporting Information

## Role of positional isomerism on A-site organic cation: structural variation driven photophysical and ferroelectric responses in centrosymmetric layered perovskites

Vishal Singh[a], Poonam Moar[b], Dirtha Sanyal[c,d], Sourabh Barua[b] and Joydeep Dhar*[a]

[a]*Department of Chemistry, Birla Institute of Technology, Mesra, Ranchi, 835215, India.*

[b]*Department of Physics, Central University of Punjab, Bathinda, 151401, India.*

[c]*Variable Energy Cyclotron Centre, 1/AF, Bidhannagar, Kolkata, 700064, India.*

[d]*Homi Bhabha National Institute, Training School Complex, Anushakti Nagar, Mumbai, 400094, India.*

*Corresponding author *E-mail address: joydeepdhar@bitmesra.ac.in*

**Table S1** Crystallographic data and structure refinement for single-layered ortho and para-fluoro NMPM-based perovskites obtained by analysing single-crystal XRD data measured at 298 K.

| | orthoF_S-1 | metaF_S-2 | paraF_S-3 |
|---|---|---|---|
| CCDC number | 2427201 | 1845548‡* | 2376464 |
| Chemical formula | $C_{16}H_{22}Br_6F_2N_2Pb_2$ | $C_{16}H_{22}Br_4F_2N_2Pb$ | $C_{16}H_{22}Br_4F_2N_2Pb$ |
| Formula weight | 1174.19 g/mol | 807.18 g/mol | 807.18 g/mol |
| Temperature | 298 K | 293 K | 293 K |
| Wavelength | 1.54178 | 0.71073 | 0.71073 |
| Crystal system | Triclinic | Orthorhombic | Orthorhombic |
| Space group | P-1 | Pbcn | Pbcn |
| Unit cell dimensions | a = 7.4391(8) Å; α = 99.917° (2) b = 7.4427(8) Å; β = 99.902° (2) c = 13.4802(15) Å; γ = 108.295(2)° | a = 7.9738(5) Å; α = 90° b = 8.8741(6) Å; β = 90° c = 32.445(3) Å; γ = 90° | a = 8.0826(6) Å; α = 90° b = 8.8187(6) Å; β = 90° c = 32.159(3) Å; γ = 90° |
| Volume | 677.35(13) $Å^3$ | 2295.8(3) | 2292.2(3) $Å^3$ |
| Z | 1 | 4 | 4 |
| Density (calculated) | 2.879 $g/cm^3$ | 2.335 $g/cm^3$ | 2.339 $g/cm^3$ |
| Absorption coefficient | 34.427 $mm^{-1}$ | 14.329 $mm^{-1}$ | 14.351 $mm^{-1}$ |
| F (000) | 524.0 | 1488 | 1488 |
| Measured Theta range | 3.430 to 68.313° | 2.846 to 25.116° | 3.419 to 24.998° |
| Absorption correction | Multi-Scan | Multi-Scan | Multi-Scan |
| Goodness-of-fit on F2 | 1.090 | 1.068 | 1.108 |
| Final indices; I>2σ(I) | R1 = 0.0558; wR2 = 0.1602 | R1 = 0.0571; wR2 = 0.1445 | R1 = 0.0674; wR2 = 0.2039 |
| All data | R1 = 0.0559; wR2 = 0.1602 | R1 = 0.0716 wR2 = 0.1579 | R1 = 0.0940 wR2 = 0.2313 |
| Largest diff. peak and hole | 3.109 and -1.534 | 1.554 and -2.002 | 2.448 and -4.734 |

$w = 1/[\sigma^2(F_o^2) + (0.0973P)^2 + 7.1224P]$ (for ortho); $w = 1/[\sigma^2(F_o^2) + (0.0790P)^2]$ (for meta); $w = 1/[\sigma^2(F_o^2) + (0.1087P)^2 + 20.9475P]$ (for para) where $P = (F_o^2 + 2F_c^2)/3$

‡ The CCDC number was from the previously reported literature.[1]

* The crystal data were from the experimentally recorded data of the prepared single crystal.

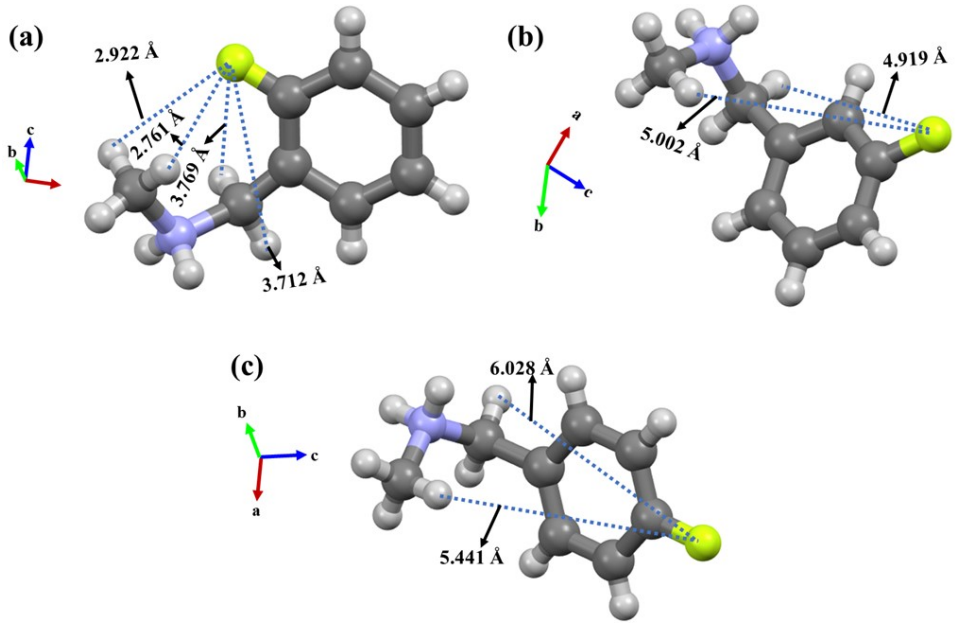


**Figure S1:** Intramolecular C-F---H-C interaction in a) orthoF b) metaF and c) paraF NMPM organic cations.

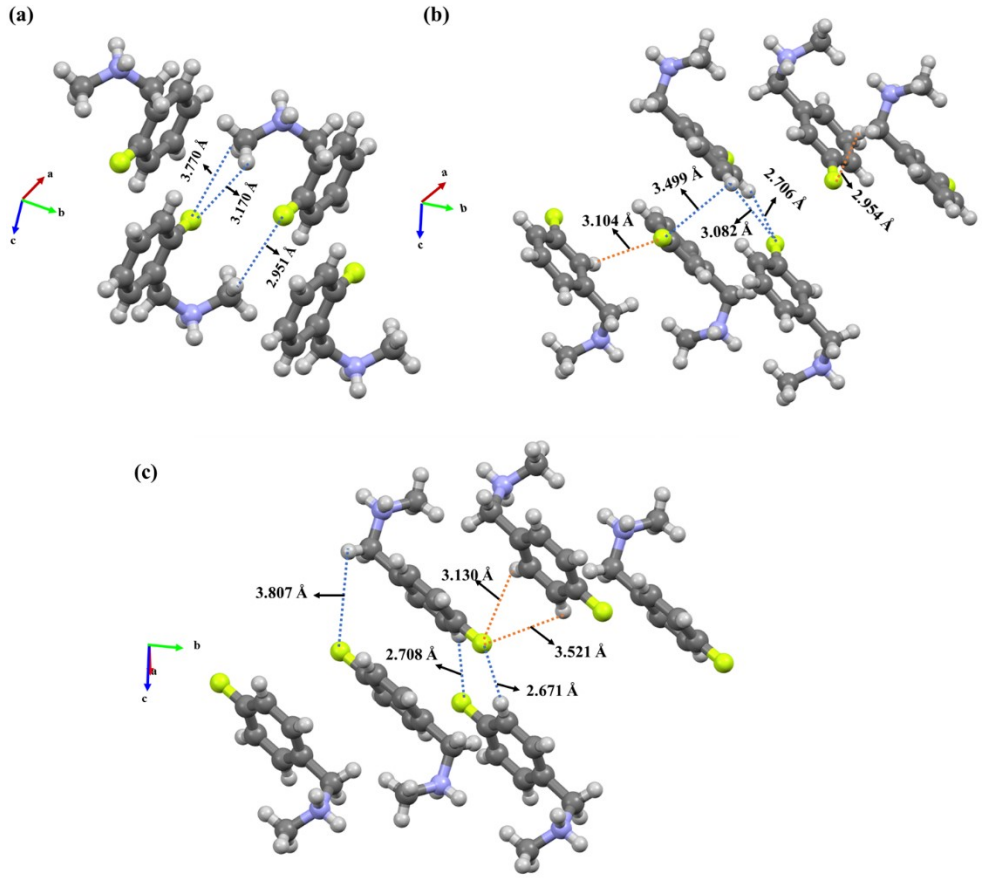


**Figure S2:** The weak intermolecular van der Waal's C–F···H–C interactions link the spacer cations into a cohesive bilayer network. Orange dashed lines show interaction between organic cations of the same layer, whereas the blue dashed line indicates the interaction between two anti-parallel organic layers.

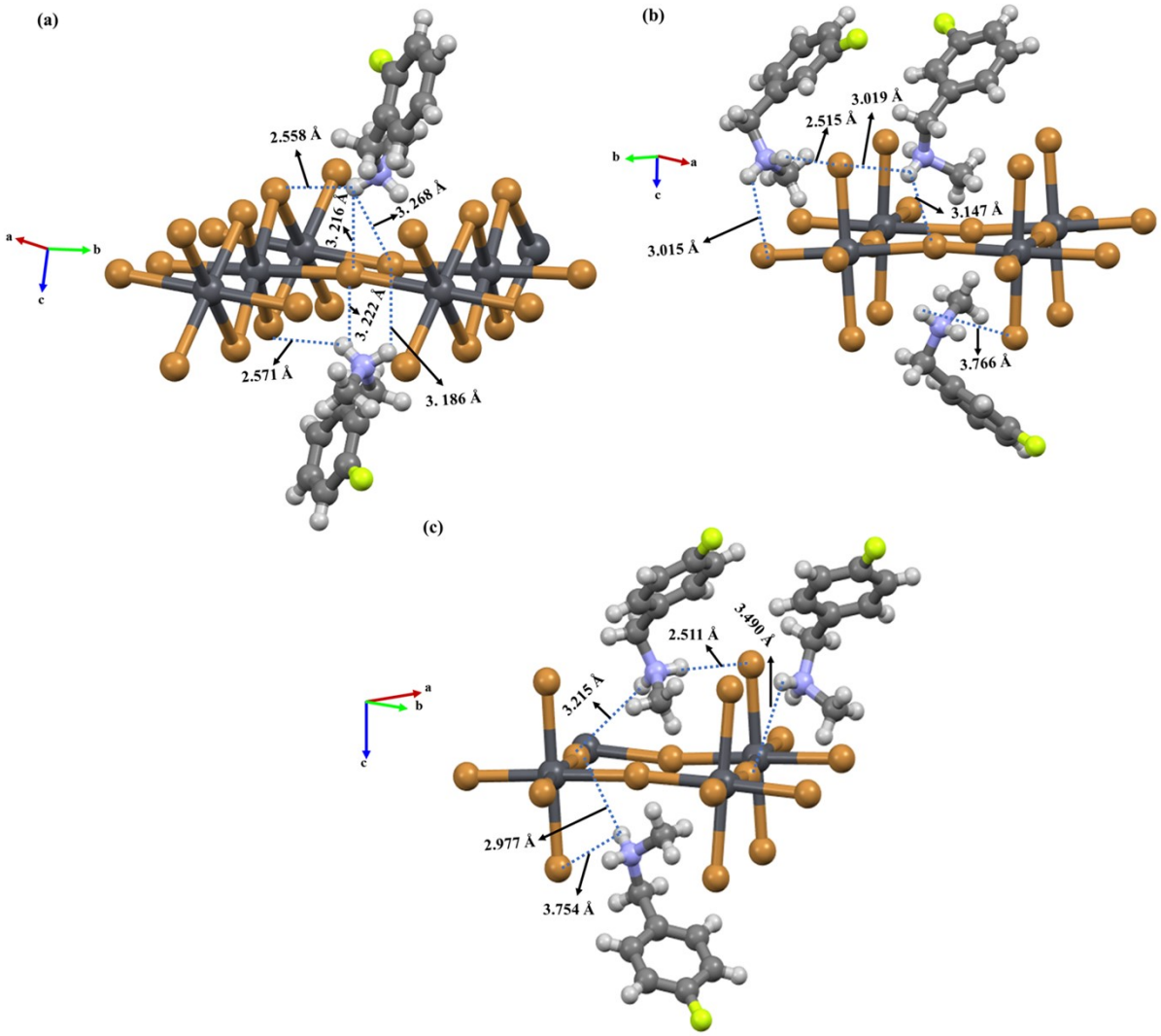


**Figure S3:** Intermolecular N-H---Br interaction in a) S-1 b) S-2 and c) S-3 showing the nearest interaction being in S-3 as compared to S-2 and S-1.

**Table S2:** Pb-Br bond lengths considered for the calculation of distortion indices in a) S-1 b) S-2 and c) S-3.

| S-1 (Å) | S-2 (Å) | S-3 (Å) |
|---|---|---|
| 3.02400 | 3.09100 | 3.07500 |
| 3.02400 | 3.09100 | 3.07500 |
| 3.03000 | 3.01000 | 3.02000 |
| 3.03000 | 3.01000 | 3.02000 |
| 3.03500 | 2.90800 | 2.93600 |
| 3.03500 | 2.90800 | 2.93600 |

**Table S3:** Br-Pb-Br bond angles considered for the calculation of angle variance in a) S-1 b) S-2 and c) S-3.

| S-1 | S-2 | S-3 |
|---|---|---|
| 86.99° | 89.78° | 90.89° |
| 86.99° | 89.99° | 94.6° |
| 87.35° | 95.6° | 89.66° |
| 87.35° | 95.6° | 90.89° |
| 88.82° | 73.87° | 89.55° |
| 88.82° | 90.47° | 94.6° |
| 91.18° | 90.47° | 89.66° |
| 91.18° | 89.99° | 75.39° |
| 92.65° | 89.73° | 89.81° |
| 92.65° | 94.92° | 89.55° |
| 93.01° | 89.73° | 89.81° |
| 93.01° | 89.78° | 95.41° |

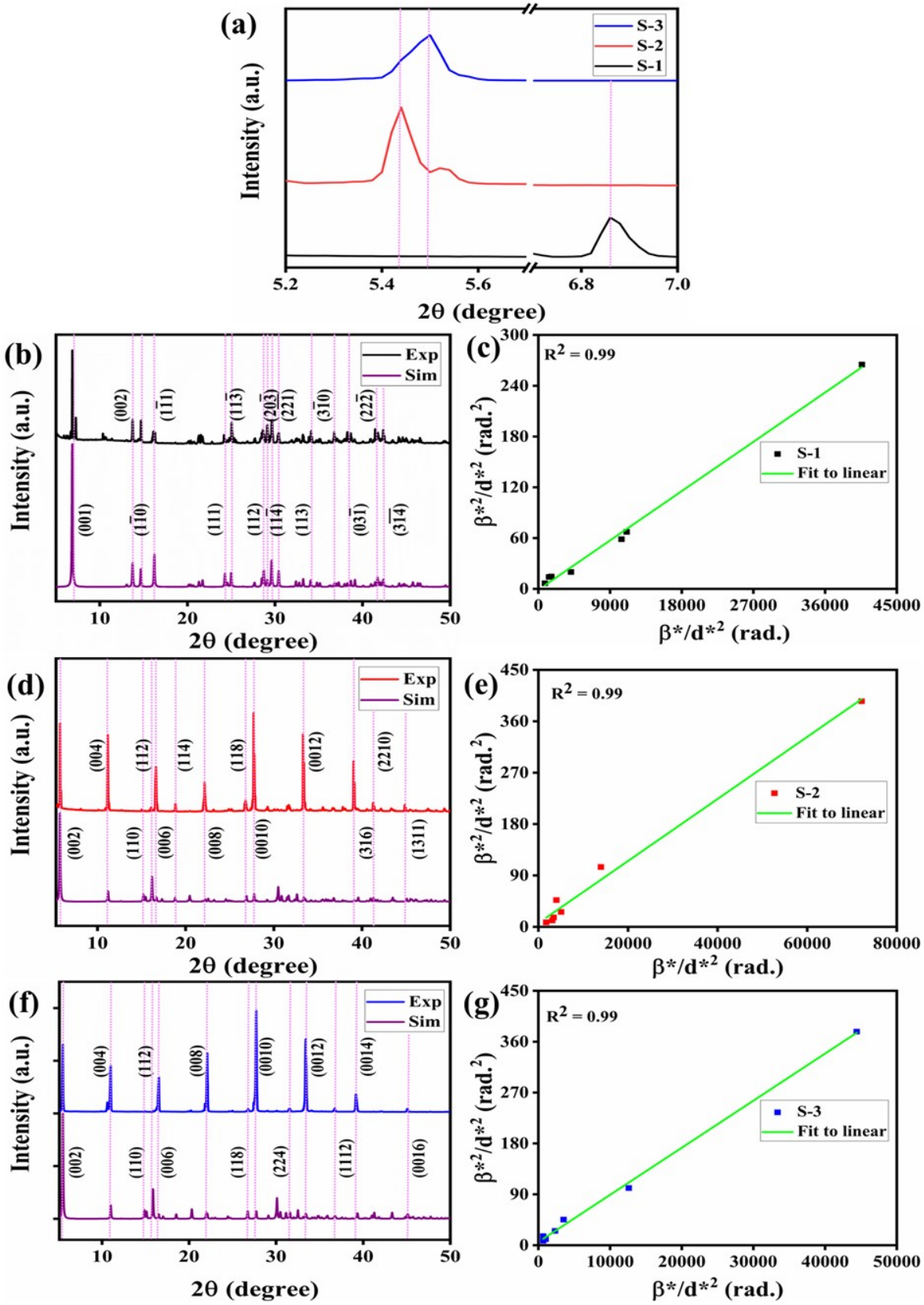


**Figure S4:** (a) Showing shifting of (002) diffraction peak of S-3 concerning S-2, for phase purity experimentally measured powder XRD spectra (Exp) compared with the simulated (Sim) in (b), (d) and (f) for S-1, S-2 and S-3, respectively. Crystallite size was calculated using Halder-Wagner Plots for S-1 (c), S-2 (e) and S-3 (g).

**Table S4:** Average crystallite size measured using PXRD

| Sample | Avg. crystallite size (nm) |
|---|---|
| S-1 | 153.85 |
| S-2 | 185.19 |
| S-3 | 120.48 |

**Table S5:** Assignment of some characteristic vibrational modes

| Vibration modes | Wavenumber ($cm^{-1}$) |
|---|---|
| N-H stretching | ~3120 |
| -$CH_2$- stretching | ~2990 |
| -$CH_3$ stretching | ~2790 |
| C-H bending (aromatic ring) | ~1580, 1514, 1450 |
| C-C stretching (aromatic ring) | ~1395 |
| C-F stretching | ~1250 |
| C-N stretching | ~1120 |

**Table S6:** Radiative ($k_{rad.}$) and nonradiative ($k_{nonrad.}$) rate constants of S-1, S-2 and S-3

| Sample | $k_{rad.}$ (x $10^6$ $s^{-1}$) | $k_{nonad.}$ (x $10^8$ $s^{-1}$) |
|---|---|---|
| S-1 | 0.2 | 0.32 |
| S-2 | 3.1 | 1.38 |
| S-3 | 4.6 | 1.03 |

The following equations were used to calculate the rate constants,[2]

$$k_{nonrad.} = (1 - \varphi)/\tau_{avg} \quad \text{.....(ES1)}$$

$$k_{rad.} = \left(1/\tau_{avg}\right) - k_{nonrad.} \quad \text{.....(ES2)}$$

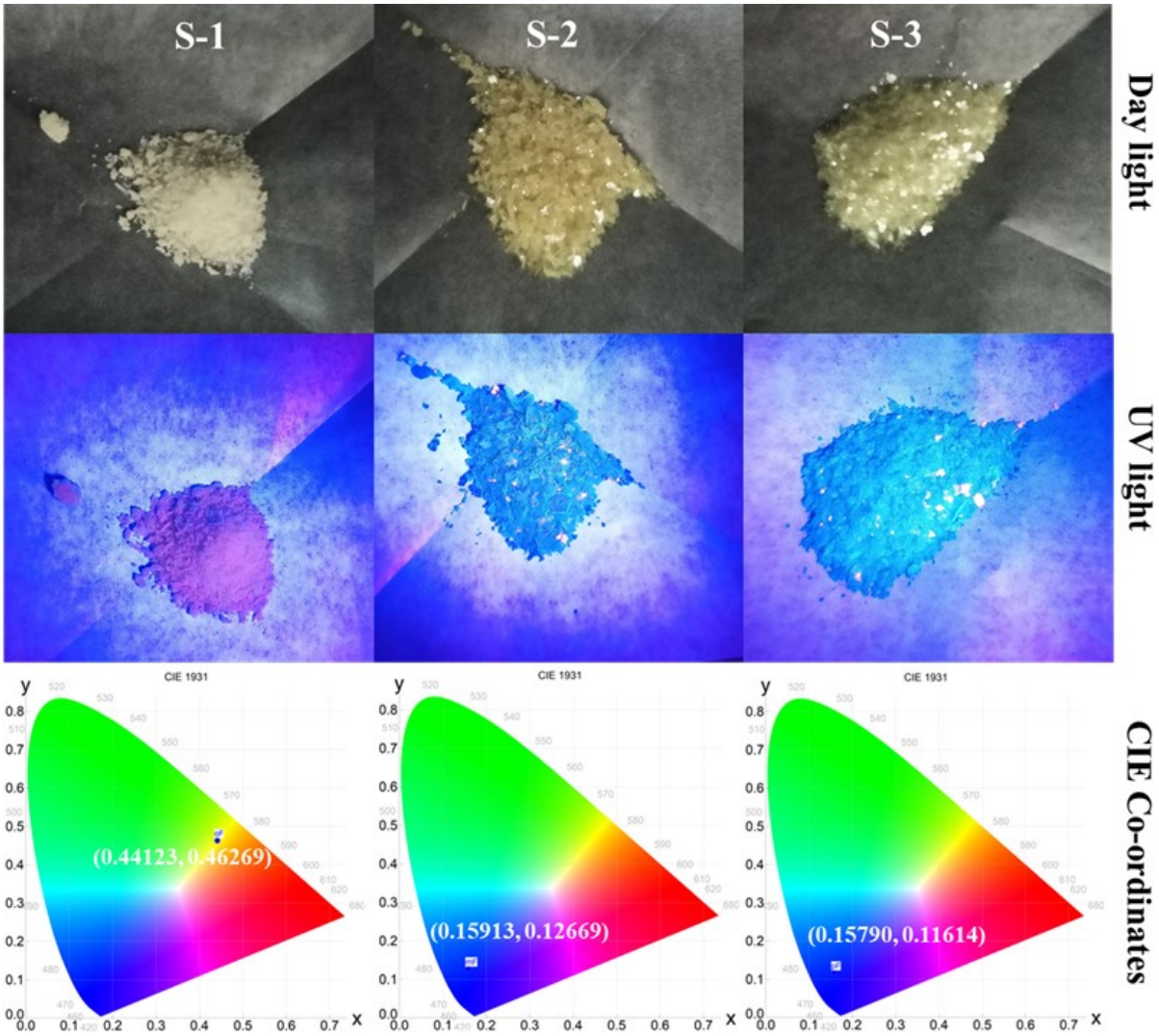


**Figure S5:** Daylight, UV light photographs and corresponding CIE-co-ordinates of each sample with S-1, S-2, and S-3 being marked as oF, mF and pF, respectively.

**Table S7:** Entropy of fusion of each of the three samples

$$\Delta S_{fusion} = \frac{\Delta H_{fusion}}{T} \quad \text{……..(ES3)}$$

| Sample | $\Delta S_{fusion}$ KJ mol$^{-1}$ K$^{-1}$ |
|---|---|
| S-1 | 0.085 |
| S-2 | 0.084 |
| S-3 | 0.109 |

**Table S8:** Fitting parameters of the equivalent circuit under dark and light conditions

| Sample | $R_1$ (Ω) | $C_1$ | $R_2$ (Ω) | Q | n |
|---|---|---|---|---|---|
| S-1 (dark) | 119 | 5.034E-10 | 1306.0 | 6.686E-5 | 0.763 |
| S-1 (light) | 115 | 5.055E-10 | 1296.3 | 7.121E-5 | 0.776 |
| S-2 (dark) | 115 | 2.529E-10 | 2530.8 | 7.683E-5 | 0.694 |
| S-2 (light) | 113 | 2.534E-10 | 2508.6 | 7.737E-5 | 0.725 |
| S-3 (dark) | 100 | 2.360E-10 | 2405.8 | 8.316E-5 | 0.681 |
| S-3 (light) | 100 | 2.394E-10 | 2380.3 | 7.729E-5 | 0.739 |

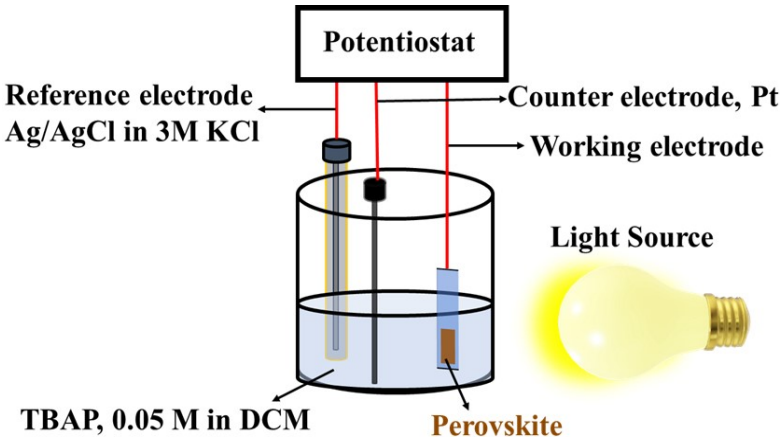


**Figure S6:** Device set-up used for performing EIS and Chronoamperometric tests.

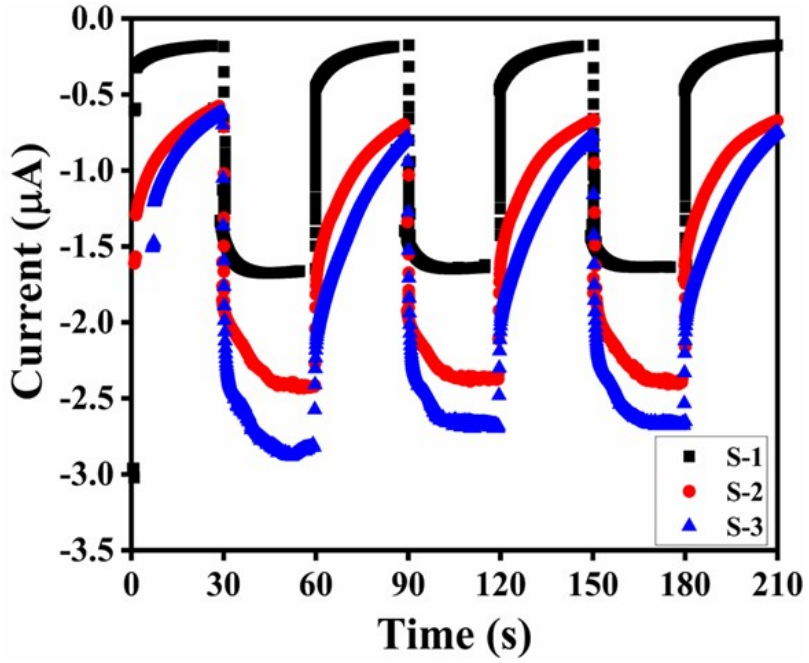


**Figure S7:** Chronoamperometric i–t curve as recorded.

$$photosensitivity = \frac{|I_D - I_L|}{I_D} \qquad \text{……..(ES4)}$$

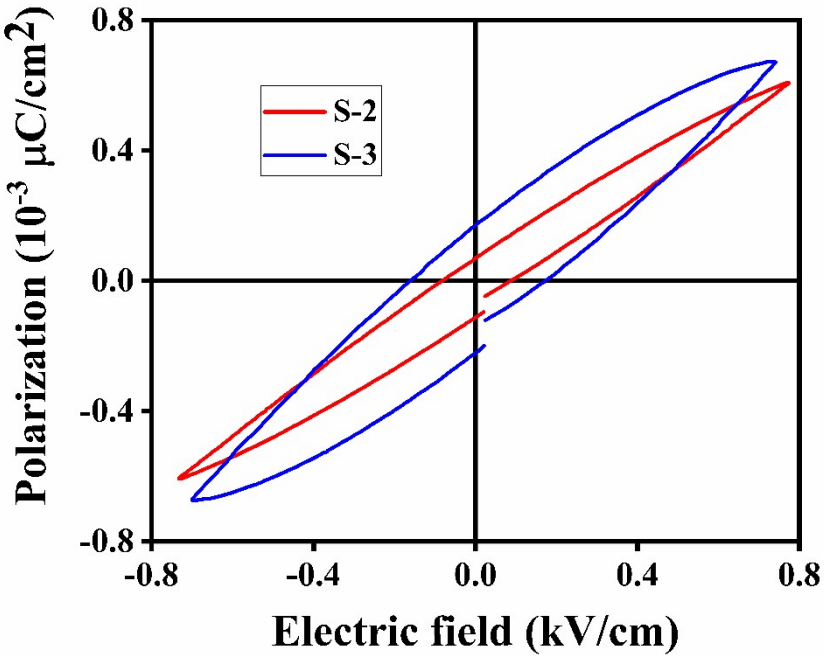


**Figure S8:** P-E loop for S-2 and S-3.

## References

1. Y. Hao, S. Wen, J. Yao, Z. Wei, X. Zhang, Z. Jiang, Y. Mei and H. Cai, *J. Solid State Chem.*, 2019, **270**, 226-230.
2. J. R. Lakowicz, *Principles of fluorescence spectroscopy*, Springer, 2006.